

Stripping Analysis of the (d,p) Angular Distributions from the $\text{Cl}^{35}(d,p)\text{Cl}^{36}$ and the $\text{Cl}^{37}(d,p)\text{Cl}^{38}$ Reactions*

A. M. HOOGENBOOM,[†] E. KASHY,[‡] AND W. W. BUECHNER

Laboratory for Nuclear Science and Department of Physics, Massachusetts Institute of Technology, Cambridge, Massachusetts

(Received March 21, 1962)

The analysis of the angular distribution of the protons from the $\text{Cl}^{35,37}(d,p)\text{Cl}^{36,38}$ reactions revealed forty-six levels in Cl^{36} and four levels in Cl^{38} , previously unreported, and the l_n values and absolute differential cross sections for fifty groups to levels in Cl^{36} and for seven groups to levels in Cl^{38} . The discussion which is given in terms of the shell model resulted in the following spin assignments: The 0.789-MeV state in Cl^{36} has $J^\pi=3^+$, and the 1.163-MeV state has probably $J^\pi=1^+$. The spins of the levels at 0.671, 0.761, and 1.309 MeV in Cl^{38} are 5^- , 3^- , and 4^- , respectively. The observed values of the single-particle reduced width θ_s^2 for the different subshells agree quite well with the values given by Macfarlane and French for other nuclei.

I. INTRODUCTION

THE stripping analysis of the (d,p) angular distributions from the $\text{Cl}^{35,37}(d,p)\text{Cl}^{36,38}$ reactions yields information on the ground-state configuration of Cl^{36} and Cl^{37} and on the single-particle levels in Cl^{36} for the $1d_{3/2}$, and on Cl^{36} and Cl^{38} for the $1f_{7/2}$, $2p_{3/2}$, and $2p_{1/2}$ subshells.

Previous work on these reactions was performed by Paris, Buechner, and Endt,¹ who identified twenty-three levels in Cl^{36} and six levels in Cl^{38} through magnetic analysis of the protons at $\theta=90^\circ$, by King and Beach,² who determined the angular distribution of the ground-state proton group in Cl^{36} , and by Teplov,³ who investigated the angular distributions for protons to Cl^{36} with photographic plates at a deuteron energy of 4 MeV. Since that work is of rather low resolution, it only revealed the distributions to the four lowest levels. No absolute cross sections were obtained.

The (n,γ) reaction on Cl^{36} has been investigated extensively by many authors,⁴ and more recently by Groshev *et al.*⁵ using a high-resolution Compton spectrometer, and by Draper and Fleischer⁶ using scintillation counters and coincidence techniques.

In the present work seventy levels could be identified in Cl^{36} below $E_x=7$ MeV and nine levels in Cl^{38} below $E_x=2$ MeV, using a gas target with carbon tetrachloride gas in its natural isotropic composition (24.6% Cl^{37} and 75.4% Cl^{36}). Angular distributions were obtained for fifty groups in Cl^{36} and for seven groups in Cl^{38} . The results are discussed in terms of the shell model. Since

the ground state of Cl^{35} is expected to be mainly $[(j^n)]_{\tau_0 J_0}=[(d_{3/2}^8)]_{1/2 3/2}$, this model predicts three $l_n=2$ proton groups to low-lying levels in Cl^{36} with $J^\pi=1^+$, 2^+ , and 3^+ . The ground state of Cl^{37} is mainly $[(d_{3/2}^5)]_{3/2 3/2}$, and therefore four of the low-lying levels in Cl^{38} are expected to be $[(d_{3/2}^5)_{3/2 3/2}(f_{7/2})_{1/2 7/2}]_{\tau J=2 J}$, with $J^\pi=2^-$, 3^- , 4^- , and 5^- , and predominantly $l_n=3$ stripping patterns. The experiments indeed showed clearly the existence of these levels, although admixtures of a lower l_n value in some groups reveal configuration mixing in the ground state of Cl^{35} and in the second excited state of Cl^{38} .

II. EXPERIMENTAL PROCEDURE AND RESULTS

The deuteron beam was obtained from the MIT-ONR electrostatic generator.⁷ The beam was analyzed with a 90-deg deflection magnet. The energy-defining slits were adjusted to 0.50 mm which would allow a maximum energy spread in the beam of 10 keV. The broad-range spectrograph^{8,9} was used for the magnetic analysis of the protons.

The target consisted of carbon tetrachloride gas. This offers two advantages over a solid target. First, absolute cross-section measurements are much easier. Second, CCl_4 has a much higher chlorine content than, for example, barium chloride has. A rotating gas cell with a very thin cylindrical window was developed. This cell permits observation of reaction particles at all angles. The gas-target system and the preparation of the thin windows have been described in detail elsewhere.¹⁰ A simple gas-handling system used to measure and to regulate the gas pressure has been described in a previous article.¹¹ The gas inlet and gas outlet (into vacuum) of the gas cell were kept slightly open during the experiment to remove organic vapor originating from rubber seals and the like.

⁷ W. W. Buechner, A. Sperduto, C. P. Browne, and C. K. Bockelman, *Phys. Rev.* **81**, 1502 (1953).

⁸ W. W. Buechner, C. P. Browne, H. A. Enge, M. Mazari, and C. D. Buntschuh, *Phys. Rev.* **95**, 609 (1954).

⁹ C. P. Browne and W. W. Buechner, *Rev. Sci. Instr.* **27**, 899 (1956).

¹⁰ A. M. Hoogenboom, *Rev. Sci. Instr.* **32**, 1395 (1961).

¹¹ E. Kashy, A. M. Hoogenboom, and W. W. Buechner, *Phys. Rev.* **124**, 1917 (1961).

* This work has been supported in part through a contract with funds provided by the U. S. Atomic Energy Commission, by the Office of Naval Research, and by the Air Force Office of Scientific Research.

[†] Now with the Instituut voor Kernfysisch Onderzoek, Amsterdam.

[‡] Now at Princeton University, Princeton, New Jersey.

¹ C. H. Paris, W. W. Buechner, and P. M. Endt, *Phys. Rev.* **100**, 1317 (1955).

² J. S. King and E. H. Beach, *Phys. Rev.* **90**, 381 (1953).

³ I. B. Teplov, *Soviet Phys.—JETP* **4**, 31 (1957).

⁴ P. M. Endt and C. M. Braams, *Revs. Modern Phys.* **29**, 683 (1957).

⁵ L. V. Groshev, A. M. Demidov, and V. N. Lutsenko, *Izvest. Akad. Nauk. S.S.S.R. Ser. Fiz.* **24**, 833 (1960).

⁶ J. E. Draper and A. A. Fleischer, *Phys. Rev.* **122**, 1585 (1961).

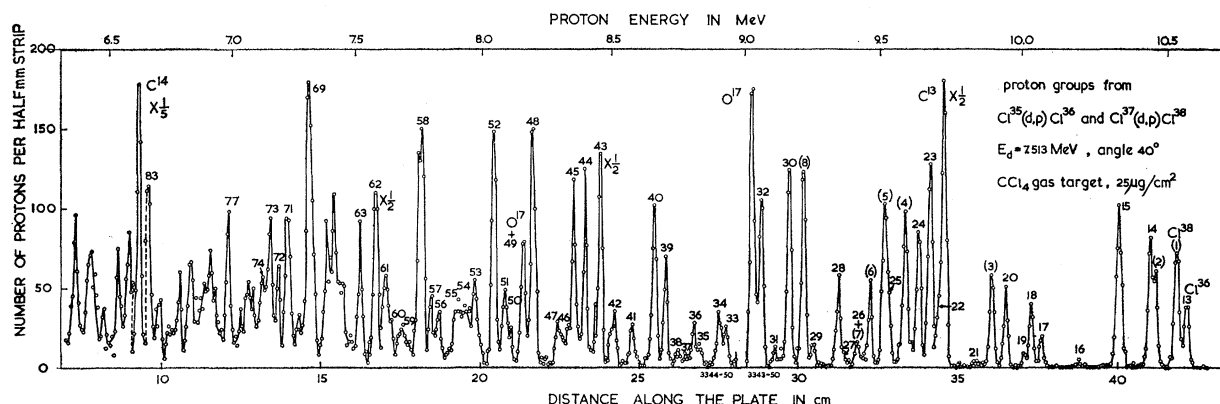


FIG. 1. Part of the proton spectrum from the $\text{Cl}^{35}(d,p)\text{Cl}^{36}$ and $\text{Cl}^{37}(d,p)\text{Cl}^{38}$ reactions. The numbers between parentheses indicate proton groups to Cl^{38} .

The target thickness in $\mu\text{g}/\text{cm}^2$ is determined by the width of the vertical entrance slit of the spectrograph, the angle of observation, and the gas pressure and temperature in the cell. In all experiments the gas pressure was 0.9 cm Hg. The target thickness was at all angles $50 \mu\text{g}/\text{cm}^2$ or less. This was achieved through appropriately setting the width of the vertical entrance slit.¹¹ For 7.5-MeV deuterons, $50 \mu\text{g}/\text{cm}^2$ is equivalent to an energy loss of about 3 keV. The target thickness in the direction of the emitted protons, which depends on the width of the vertical exit slits of the deflection magnet, as well as on such factors as the gas pressure, etc., was also less than $50 \mu\text{g}/\text{cm}^2$. For 10-MeV protons, this is equivalent to an energy loss of about 1 keV or less.

The photographic plates used with the broad-range spectrograph⁹ to detect the protons were covered with a sufficiently thick layer of aluminum to stop the elastically and inelastically scattered deuterons. Part of the proton spectrum obtained at a reaction angle of 40 degrees is shown in Fig. 1. Other measurements were performed at 5, 10, 20, 25, 32.5, 40, 47.5, 55, 70, 90, and 130 deg. Every measurement resulted in the determination of the absolute differential cross section. No renormalization was found necessary, since the target thickness of the gas target was almost independent of the beam current. The measurements were performed at a deuteron energy of 7.513 MeV. The deuteron energy was measured by observing the elastically scattered deuterons using an uncovered zone of the photographic plates. This measurement was done at several angles.

The Q values obtained from the analysis of the 10-, 40-, 90-, and 130-deg data are given in Tables I and II for the $\text{Cl}^{35}(d,p)\text{Cl}^{36}$ and $\text{Cl}^{37}(d,p)\text{Cl}^{38}$ reactions, respectively. The results of this work are in excellent agreement with that of Paris *et al.*,¹ represented in the third column. The level in Cl^{38} that they reported at 2.219 MeV was not observed in the present analysis. A weak group at this energy in the 90-deg spectrum (the work of Paris *et al.* was performed at this angle) shifted as a function of angle with respect to the Cl^{38} groups (4)

and (5) and might be a weak Cl^{36} group. The excitation energies are given in the fourth column of the Tables I and II. The figure in parentheses following the excitation energies is the standard error in keV. The analysis of the region of Q values larger than 2.3 MeV revealed all proton groups with an intensity stronger than about half the intensity of the Cl^{36} group (19), unless such a group was within 15 keV of a strong group. Since the level density from $Q=2.3$ MeV down increases rapidly, many weak groups in this region certainly escaped observation. Many Cl^{38} levels might have been missed, because Cl^{38} is about a factor of 3 less abundant than Cl^{36} . In fact, no Cl^{38} groups were observed with Q values less than 1.9 MeV, although a group with an intensity of the order of the Cl^{38} group (7) would probably have been identified. In the region above Cl^{36} group (60), there was a strong indication of some Cl^{38} groups. This complicated the analysis of the Cl^{36} groups in this region. Several could not be analyzed and are omitted from Table I. The numbering in column 1 indicates their omission.

The maximum differential cross sections are listed in the fifth column. Since it is not clear whether these values have to be corrected for an "isotropic compound-nucleus background" to obtain the stripping part of the total differential cross section, generally no such correction was applied. The error in the cross-section values is about 7%, because of the errors in the charge, pressure, and solid-angle measurements, and the uncertainty in the gas temperature. For cross sections in Cl^{36} less than 1 mb/sr, a statistical error has to be added. This increases the total error from 7% at 1 mb/sr to 15% at 0.1 mb/sr. The distributions of very weak groups have not been analyzed, since they are not of interest in connection with a stripping analysis. Above Cl^{36} group (71), some of the stronger groups could not be analyzed.

Groshev *et al.*⁵ had to assume levels at 4.138, 4.757, 5.016, 5.516, and 6.344 MeV in order to explain a number of the 63 gamma-ray groups they observed in their study of the $\text{Cl}^{35}(n,\gamma)\text{Cl}^{36}$ reaction. These levels

TABLE I. Summary of results for the levels of Cl^{36} .

Level	Q value ± 0.008 (MeV) This work	Reference 1	E_x (in MeV) ^a	$\left(\frac{d\sigma}{d\Omega}\right)_{\text{max}}$ mb/sr (lab)	θ_p (deg) (lab)	l_n	$(2J+1)\theta^2$ Adjusted R	$(2J+1)\theta^2$ R=5.7 F
0	6.354	6.354		$\leq 0.66^b$	31	0		$\leq 0.0021^b$
1	5.565	5.564	0.789(4)	0.89	30	2		0.041
2	5.191	5.191	1.163(4)	0.38	0	0		0.016
3	4.755	4.754	1.599(5)	1.72	32	2		0.0053
4	4.400	4.402	1.954(5)	$\leq 0.18^c$	0	0		$\leq 0.0074^c$
5	3.882	3.881	2.472(6)	0.90	0	0		0.0027
6	3.857	3.856	2.497(6)	4.2	0	0		0.013
7	3.832	3.831	2.522(6)	≤ 0.8 or	30-45	2 or		≤ 0.03 or
8	3.675	3.670	2.679(6)	≤ 0.6		3		≤ 0.06
9	3.538	3.534	2.816(6)	3.10 ^d	20	1	0.043	0.036
10	3.486	3.482	2.868(6)	1.13	0	0		0.0034
11	3.454	3.449	2.900(6)	1.47	43	3		0.133
12	3.354	3.350	3.000(6)	0.13	(0)	3		0.056
13	3.251	3.244	3.103(7)	0.63	43	3		0.022
14	3.142	3.140	3.212(6)	0.25	42	3		0.044
15	3.016	3.013	3.338(6)	4.05	19	1	0.055	0.028
16	2.880	2.880	3.474(7)	2.56	18	1	0.035	0.028
17	2.748	2.748	3.606(7)	0.14	22	1	0.002	0.022
18	2.714	2.710	3.640(6)	0.25	45	3		0.017
19	2.684	2.681	3.670(8)	1.61	19	1	0.022	0.059
20	2.626	2.622	3.728(7)	5.75	19	1	0.077	0.059
21	(2.523)		(3.831)	0.16	15	1	0.0021	0.0016
22	2.384	2.384	3.970(7)	0.27	16	1	0.0036	0.0026
23	2.354	2.351	4.000(7)	1.64	20	1	0.022	0.016
24	2.314	2.311	4.040(7)	0.07	30-60			0.023
25	2.208		4.146(7)	0.28	40	3		0.023
26	(2.085)		(4.269)	weak				0.018
27	(2.054)		(4.300)	1.99	18	1	0.027	0.031
28	2.031		4.323(7)	3.34	18	1	0.045	0.029
29	1.941		4.413(8)	3.16	19	1	0.042	0.011
30	1.850		4.504(7)	1.27	20	1	0.017	0.011
31	1.794		4.560(8)	weak				0.013
32	1.747		4.607(8)	weak				0.029
33	1.620		4.734(8)	weak				0.024
34	1.589		4.765(8)	3.5 \pm 1.0 ^e	18	1	0.046	0.029
35	1.520		4.834(8)	0.75	0	0		0.024
36	1.497		4.857(8)	2.94	19	1	0.039	0.012
37	1.467		4.887(8)	0.16	40-50	3		0.0057
38	1.435		4.919(8)	0.71	15-20	1	0.0092	0.0057
39	1.389		4.965(8)					
40	1.346		5.008(8)					
41	1.264		5.090(8)	1.04	17	1	0.014	0.0079
42	1.194		5.160(8)	1.38	18,55	1	0.018	0.010
43	1.141		5.213(8)	0.46	17	1	0.006	0.0034
44	1.085		5.269(8)	1.01	19	1	0.013	0.0072
45	1.040		5.314(8)	6.1	16	1	0.079	0.044
46	1.015		5.339(8)	2.75	17	1	0.036	0.019
47	0.978		5.376(8)	2.71	18	1	0.035	0.019
48	0.885		5.469(8)					
49	0.836		5.518(8)					
50	0.804		5.550(8)					
51	0.770		5.584(8)					
52	0.732		5.622(8)					
53	0.653		5.701(8)	0.23	17	1	0.0030	0.0014
54	0.623		5.731(8)	0.91	17	1	0.012	0.0056
55	0.588		5.766(8)	0.62	18	1	0.0080	0.0038
56	0.518		5.836(8)	0.94	17	1	0.012	0.0057
57	0.483		5.871(8)	0.55	15	1	0.0071	0.0032
58	0.448		5.906(8)	0.59	18	1	0.0076	0.0034
59	0.402		5.952(8)	4.74	17	1	0.062	0.027
60	0.382		5.972(8)					
61	0.322		6.032(8)					
62	0.264		6.090(8)					
63	0.199		6.155(8)	4.95	16	1	0.064	0.026
"69"	-0.002		6.356(8)	1.31	17	1	0.017	0.0067
"71"	-0.091		6.445(8)	3.73	17	1		
"72"	-0.120		6.474(8)	1.92	17	1		
"73"	-0.156		6.510(8)					
"74"	-0.192		6.546(8)					
"77"	-0.326		6.680(8)					
"83"	-0.653		7.007(8)	1.46	17	1		

^a Figure in parentheses is error in keV.^b Lower limit is 0.5 mb/sr, $(2J+1)\theta^2=0.0016$ (see text).^c Lower limit is 0.12 mb/sr, $(2J+1)\theta^2=0.005$ (see text).^d Includes the $\text{Cl}^{37}(d, p)\text{Cl}^{38}$ ground-state group.^e Large error from O^{17} ground-state contamination.

TABLE II. Summary of results for the levels of Cl^{38} .

Level	Q value ± 0.008 (MeV)		E_x (in MeV) ^a	$\left(\frac{d\sigma}{d\Omega}\right)_{\max}$ (mb/sr (lab))	θ_p (deg) (lab)	l_n	$(2J+1)\theta^2$ Adjusted R	$(2J+1)\theta^2$ R=5.7 F
0	3.878	3.877	0	1.6(40°)	≤ 40	(3)		(≤ 0.14)
1	3.207	3.205	0.671(5)	2.25	45	3		0.20
2	3.117	3.115	0.761(5)	2.30	18	1	0.031	0.024
3	2.569	2.565	1.309(6)	0.83	40	3		0.070
4	2.256	2.257	1.622(6)	1.35	45	3		0.11
5		2.219		9.7	18	1	0.129	0.089
6	2.183		1.695(6)	8.9	17	1	0.118	0.079
7	2.130		1.748(7)	3.7	17	1	0.045	0.032
8	2.089		1.789(8)	weak				
9	1.892		1.986(7)	11.7	18	1	0.156	0.102

^a Figure in parentheses is error in keV.

can be identified with the levels (25), (34), (40), (49), and (69) of Table I. They assumed also a level at 4.589 MeV. This level is not observed in the present work. They found, furthermore, a strong indication for a doublet structure of level (4). This point is further discussed in the next section.

III. STRIPPING ANALYSIS

The important information that can be extracted from stripping data is the maximum differential cross section $(d\sigma/d\Omega)_{\max}$ and the reaction angle θ_p at which this maximum occurs. The value of $(d\sigma/d\Omega)_{\max}$, through an appropriate stripping theory, is related to the dimensionless reduced width θ^2 . If the simple Butler theory¹² is used, the ratio $(d\sigma/d\Omega)_{\max}/(2J+1)\theta^2$, where J is the spin of the final state, can be easily calculated using tables prepared by Enge and Graue.¹³ These tables are based on the non-Coulomb formula given by

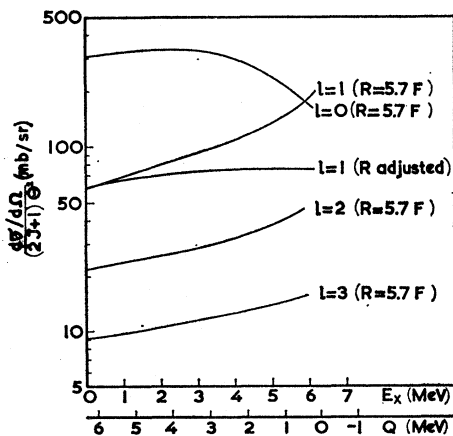


FIG. 2. Differential cross section divided by $(2J+1)\theta^2$ from the Butler theory for different values of l_n with $R=5.7$ F. For the $l_n=1$ "R adjusted" curve, see text.

¹² S. T. Butler, Proc. Roy. Soc. (London) **A208**, 559 (1951).

¹³ H. A. Enge and A. Graue, *Numerical Calculation of Non-Coulomb Stripping Cross Section* (Universiteti Bergen, Arbok, 1955).

Friedman and Tobocman.¹⁴ The results for the $\text{Cl}^{35}(d,p)\text{Cl}^{36}$ reaction with deuteron energy of 7.5 MeV are given in Fig. 2. The curves have been calculated for values of the orbital angular momentum of the captured neutron $l_n=0, 1, 2$, and 3, using the Gamow-Critchfield nuclear radius $R_G=(1.7+1.22 A^{1/3})=5.7$ F. The angle θ_p depends on Q and the nuclear radius R . It is customary to use R as an adjustable parameter¹⁵ to fit the theoretical value of θ_p with the observed angle. In the present analysis, the Gamow-Critchfield value offered a good fit for the distributions with $l_n=2$ and 3. The $l_n=1$ groups could not be fitted with a single value of R .

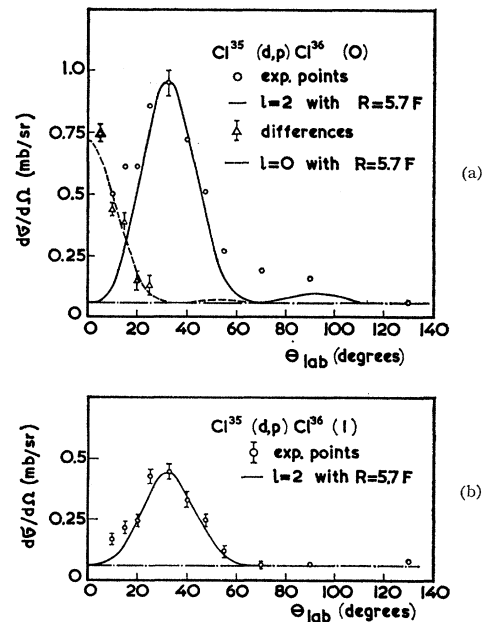


FIG. 3. The analysis of the angular distributions of $\text{Cl}^{35}(d,p)\text{Cl}^{36}$ groups (0) and (1). The Butler curves are calculated with $R=5.7$ F.

¹⁴ F. L. Friedman and W. Tobocman, Phys. Rev. **92**, 93 (1953).

¹⁵ M. H. Macfarlane and J. B. French, Revs. Modern Phys. **32**, 567 (1960).

According to the simple Butler theory, with a constant value of R , θ_p should decrease rather rapidly from 18 deg at $E_x=0$ to zero deg at $E_x \approx 5.3$ MeV. In fact, the observed θ_p for all groups is 18 ± 2 deg. Therefore, a second $l_n=1$ curve is given in Fig. 2 which is calculated with R adjusted as a function of E_x . The function $R(E_x)$ is chosen such that $\theta_p=18$ deg, independent of E_x . In a previous article,¹⁶ it has been shown that this procedure is rather dangerous, since $R(E_x)$ decreases rapidly with E_x . For example, at $E_x \approx 5.3$ MeV, $R \approx 2.6$ F. In reference 16, it is shown that both θ_p and the shape of the observed angular distributions indicate that not R but Q should be used as an adjustable parameter Q_{adj} . It is also shown there that Q_{adj} should be given a constant value of 6.3 MeV. However, since neither of the two adjustment procedures has been theoretically justified,¹⁷ and since $(d\sigma/d\Omega)_{\text{max}}/(2J+1)\theta^2$ calculated with adjusted R or with adjusted Q is about the same, the "adjusted R " method will be used in the present work to calculate $(2J+1)\theta^2$. The values of $(2J+1)\theta^2$, using a constant value of $R=5.7$ F, are also given in Tables I and II.

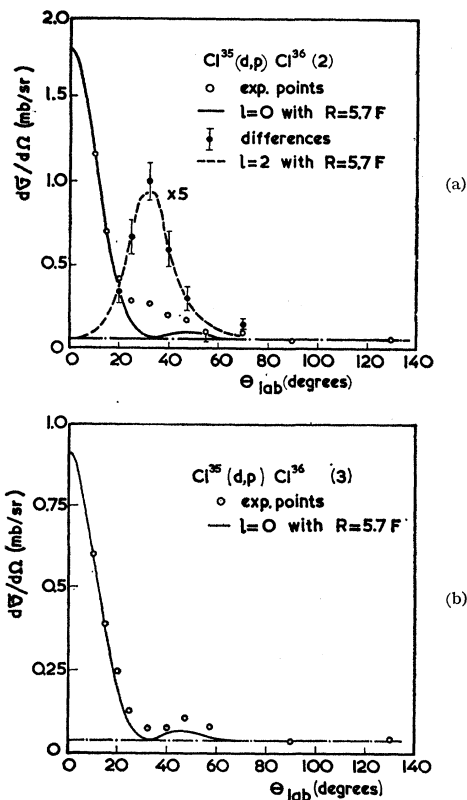


FIG. 4. The analysis of the angular distributions of $\text{Cl}^{35}(d,p)\text{Cl}^{36}$ groups (2) and (3). The Butler curves are calculated with $R=5.7$ F.

¹⁶ A. M. Hoogenboom, E. Kashy, and W. W. Buechner, *Proceedings of the Rutherford Jubilee International Conference* (Heywood and Company, Ltd, London, 1961), p. 589.

¹⁷ A. M. Hoogenboom, *Proceedings of the Rutherford Jubilee International Conference* (Heywood and Company, Ltd, London, 1961), p. 472.

In the following paragraphs, the analysis of the observed distributions will be discussed.

The $l_n=2$ Groups

The groups (0) and (1) in the summary of the results for the $\text{Cl}^{35}(d,p)\text{Cl}^{36}$ reaction are rather pure $l_n=2$. However, comparison of Figs. 3(a) and 3(b) shows that the ground-state group has a weak $l_n=0$ admixture. The analysis is given in terms of Butler curves. The $l_n=0$ admixture in the ground-state group is 0.66 mb at zero deg. Since $l_n=2$ Butler curves cannot be trusted at small angles, the figure for the $l_n=0$ admixture must be considered an upper limit. For the group (1), the $l_n=0$ admixture is ≤ 0.1 mb. A lower limit for the $l_n=0$ admixture in the ground-state group is found if the observed distribution to level (1) is used as an empirical pure $l_n=2$ curve. The lower limit for the ground-state $l_n=0$ admixture is 0.5 mb.

The group (2) in Cl^{36} is also a mixture of $l_n=0$ and $l_n=2$. This is clear from a comparison of Figs. 4(a) and 4(b). In this case, an upper and lower limit for the $l_n=2$ admixture in group (2) can be obtained; namely, $0.12 \leq (d\sigma/d\Omega)_{\text{max}} \leq 0.18$ mb. The $l_n=2$ admixture in group (3) is ≤ 0.03 mb.

The $l_n=0$ Groups

In addition to the $l_n=0$ group (3) discussed above, three more $l_n=0$ groups have been observed in Cl^{36} . The groups (6) and (31) are shown in Fig. 5. Both groups are pure $l_n=0$. The group (4) in Cl^{36} is shown in Fig. 6. Unfortunately, this group is not observed at 25

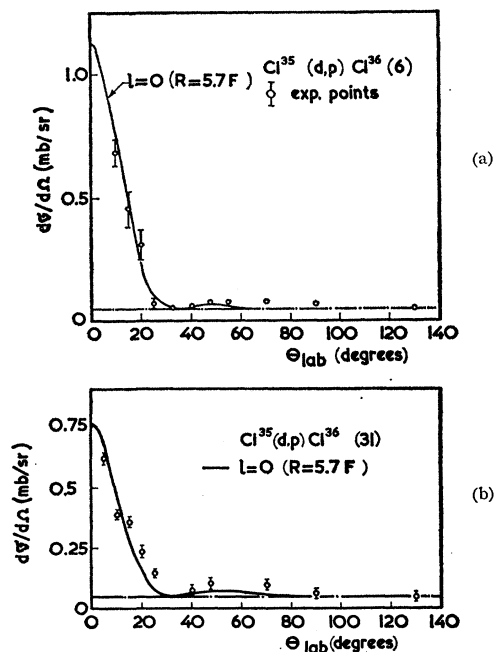


FIG. 5. The analysis of the angular distributions of $\text{Cl}^{35}(d,p)\text{Cl}^{36}$ groups (6) and (31). The Butler curves are calculated with $R=5.7$ F.

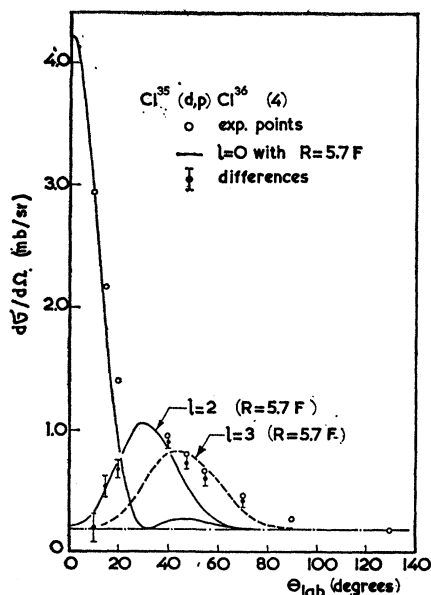


FIG. 6. The angular distribution of $\text{Cl}^{35}(d,p)\text{Cl}^{36}$ group (4). The difference points are obtained by subtracting an appropriate $l_n=0$ contribution from the experimental distribution. The $l_n=2$ and $l_n=3$ Butler curves show that the difference points can be a mixture of $l_n=2$ and 3.

and 32.5 deg, since it happened to fall at these angles in the gap between two photographic plates. The analysis is further complicated because there is good evidence that this level is actually a close doublet with a separation of 7 keV.⁵ This could not be verified in the present experiment. The analysis reveals a strong $l_n=0$ with probably an $l_n=2$ admixture combined with an $l_n=3$ contribution from the other level. The dots in

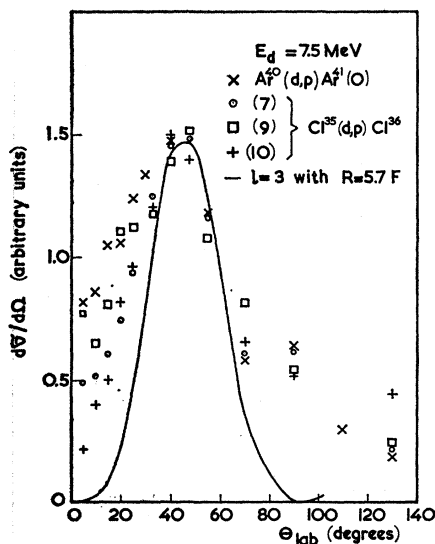


FIG. 7. The angular distributions of the $\text{Cl}^{35}(d,p)\text{Cl}^{36}$ groups (7), (9), and (10). The pure $l_n=3$ ground-state group from $\text{Ar}^{40}(d,p)\text{Ar}^{41}$ is shown for comparison. The Butler curve is calculated with $R=5.7 F$. The curves are normalized at θ_p .

Fig. 6 are differences between the experimental points and the $l_n=0$ contribution, which is calculated from Butler theory. The shape of this residue indicates the presence of about equally strong $l_n=2$ and $l_n=3$ contributions with $(d\sigma/d\Omega)_{\max} \approx 0.4$ mb for both. The $l_n=2$ and $l_n=3$ curves in Fig. 6 show that the upper limits for the $l_n=2$ and $l_n=3$ contributions are 0.8 and 0.6 mb, respectively.

The very weak group (8) is probably also $l_n=0$. However, the peak has its half-height at 40 deg and is therefore not pure stripping.

The $l_n=3$ Groups

The groups (7), (9), and (10) in Cl^{36} are certainly $l_n=3$. However, the observed distributions differ rather strongly from an $l_n=3$ Butler curve. This is shown in Fig. 7, where the three distributions are given, normalized at about 45 deg. The drawn line is the Butler curve. In Fig. 7 is also given the distribution of the pure $l_n=3$ ground-state group from the $\text{Ar}^{40}(d,p)\text{Ar}^{41}$ reaction; $Q=3.874$ MeV (reference 11). This measurement was also performed at $E_d=7.5$ MeV, and the Q values of this group and group (7) of Cl^{36} are almost the same. The fact that the shape of the Ar^{41} group resembles strongly the shape of group (7), (9), and (10) indicates that the differences between these groups and the Butler curve at about 20 degrees cannot be ascribed to $l_n=1$ admixtures.

The group (13) in Cl^{36} is shown in Fig. 8. Since it shows peaks at 20 and 45 deg, it is very probably an $l_n=1$, $l_n=3$ mixture. The analysis given in Fig. 8 is obtained using the shape of the $l_n=1$ group (12) and the $l_n=3$ group (7).

Four $l_n=3$ groups have been observed in Cl^{38} . The results are given in Fig. 9. The group (0) could only be observed at angles larger than 40 deg, since at the other angles it coincided with group (5) of Cl^{36} . Since J^π of the ground state is 2^- , this group can be a mixture of $l_n=1$ and $l_n=3$. Therefore, the only information that can be extracted from the experimental result is $(d\sigma/d\Omega)_{\max}$, $l_n=3 \leq 1.6$ mb. The groups (1) and (3) are given in Fig. 9(b). The full line in this figure is the mean

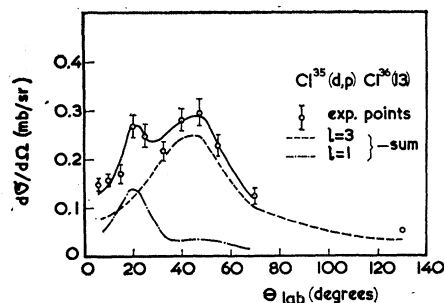


FIG. 8. The analysis of the angular distribution of the $\text{Cl}^{35}(d,p)\text{Cl}^{36}$ group (13) using the shape of the $l_n=1$ group (12) (dot-dashed curve) and the $l_n=3$ group (7) (dashed curve). The sum of these curves is the drawn line.

of the four $l_n=3$ groups given in Fig. 7. This curve shows that the groups (1) and (3) of Cl^{38} are probably pure $l_n=3$. The group (2) is given in Fig. 9(a). This group is a mixture of $l_n=1$ and $l_n=3$. The analysis given in this figure is made using the experimental result from the $l_n=1$ group (12) in Cl^{36} and the $l_n=3$ mean curve given in Fig. 9(b). The result is $(d\sigma/d\Omega)_{\max}, l_n=1=2.30$ mb and $(d\sigma/d\Omega)_{\max}, l_n=3=0.83$ mb.

The $l_n=1$ Groups

In Cl^{36} , 36 $l_n=1$ groups were found. Above $E_x=4.75$ MeV, no other than $l_n=1$ groups were observed. However, it might well be that, because of the large number of strong $l_n=1$ groups in this region, many other groups escaped observation. The shape of group (12), which is shown in Fig. 9(a), is typical for most of the $l_n=1$ Cl^{36} groups.¹⁷ They all have a first maximum at about 18 deg and a second maximum at about 50 deg which has an intensity between 25 and 30% of the first maximum. A curve which is an exception to this rule is the group (40) shown in Fig. 10(a).

The group (5) in Cl^{36} is shown in Fig. 10(b). In the same figure and on the same scale (intensity-wise) is shown the group (0) of Cl^{38} . As mentioned above, this

group almost coincides with the group (5) for $\theta \leq 40^\circ$. For these angles, the sum of (0) and (5) is given. The sum curve is clearly an $l_n=1, l_n=3$ mixture. However, since both groups may be mixtures of $l_n=1$ and $l_n=3$, no further decomposition of the sum curve is possible on the basis of the results given in Fig. 10(b). If it is assumed that the group (0) is pure $l_n=1$, a lower limit of 1.5 mb is obtained for the $l_n=1$ strength of group (5). The upper limit is 3.1 mb.

In Cl^{38} , four $l_n=1$ groups were observed. The shapes of the curves are almost identical to the shape of Cl^{36} group (12) in Fig. 9(a).

IV. DISCUSSION

Cl^{36}

The ground-state spin of Cl^{35} is $3/2^+$.⁴ According to the shell model, the main component of the ground-state wave function is $[(j^n)]_{T_0, J_0} = [(d_{3/2}^8)]_{1/2, 3/2}$. Using the notation of Macfarlane and French,¹⁵ the strong $l_n=2$ transitions to levels in Cl^{36} are indicated in Fig. 11. Thus, transitions to levels in Cl^{36} with $J^\pi=1^+, 2^+$, and 3^+ are expected; whereas the $J^\pi=0^+$ will not be observed, since it has $T=2$. Because of their angular momenta and parities, only the levels with $J^\pi=1^+$ and 2^+ can be

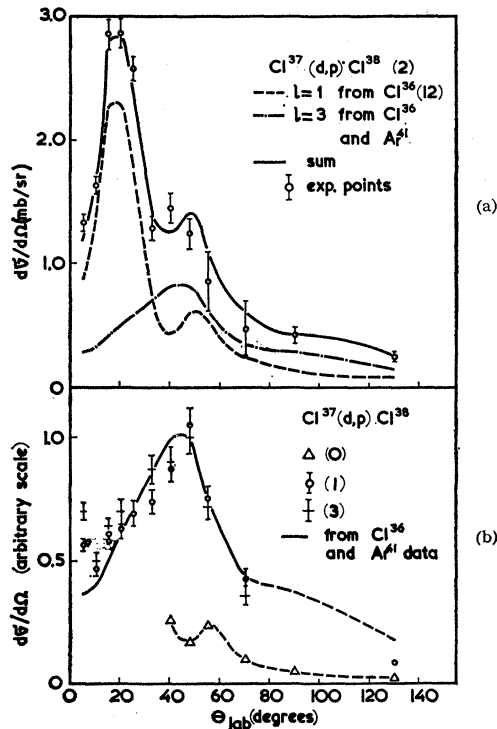


FIG. 9. (a) The analysis of $\text{Cl}^{37}(d,p)\text{Cl}^{38}$ group (2) using the shape of the $l_n=1$ group (12) of Cl^{36} (dashed curve) and the shape of the mean curve of the $l_n=3$ distributions shown in Fig. 7 (dot-dashed curve). The sum of these curves is the drawn line. (b) The angular distributions of the $\text{Cl}^{37}(d,p)\text{Cl}^{38}$ groups (1) and (3), and of group (0) for $\theta \geq 40$ deg. The drawn line is the mean curve through the distributions given in Fig. 7, normalized at θ_p with groups (1) and (3).

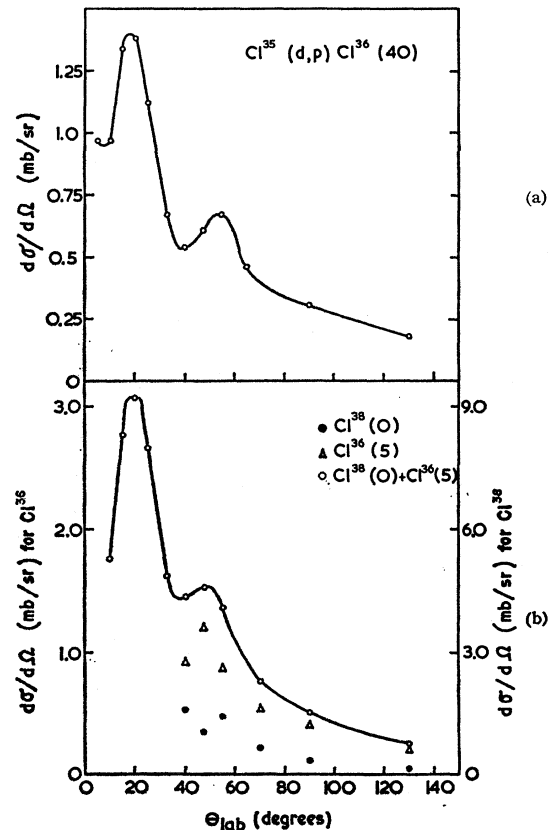
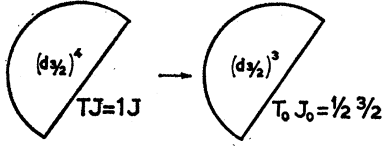


FIG. 10. (a) The angular distribution of $\text{Cl}^{35}(d,p)\text{Cl}^{36}$ group (40). (b) Experimental data on the proton groups $\text{Cl}^{38}(0)$ and $\text{Cl}^{36}(5)$.

FIG. 11. $l_n=2$ transitions to levels in Cl^{36} .

admixed with $l_n=0$. Indeed, one group, that associated with level (1), is found to be pure $l_n=2$. The ground-state spin of Cl^{36} is 2^+ .⁴ The group (2) is $l_n=2$ with a strong $l_n=0$ admixture. Therefore, level (1) is almost certainly 3^+ and level (2), 1^+ . To check these assignments further, an analysis will be made of the reduced width θ^2 , which can be written as¹⁵

$$\theta^2 = S\theta_0^2, \quad (1)$$

where S is the spectroscopic factor depending only on the nuclear wave functions, and θ_0^2 is the single-particle reduced width. The value of θ_0^2 is expected to be independent of J for a transition in a particular subshell, and it can be calculated with Eq. (1) from the experimental θ^2 if S is known. The value of S for the transition represented in Fig. 11 can be calculated using Eq. (III.70) of reference 15. The results are given in Table III. Since the values of $\theta_0^2(d_{3/2})$ given in the last column of Table III are almost equal, it can be concluded that the spin assignments given above are correct. The spin assignments to the levels (1) and (2) in Cl^{36} are in disagreement with the conclusions of Draper and Fleischer⁶ from (n,γ) work. However, since their assignments are solely based on gamma-ray transition probabilities, it is felt that a study of (γ,γ) angular correlations will be necessary to investigate this point further.

The values of θ_0^2 found are about a factor of 3 smaller than other values in the $1d$ shell (see Fig. 57, reference 15). This indicates that the ground-state wave function of Cl^{36} is not pure $[(d_{3/2}^3)]_{1/2 \ 3/2}$ but should in fact be described as shown in Fig. 12.

The summations (i,n) and (j,m) extend to all combinations of σ and ϵ which couple to $(T_0 J_0) = (\frac{1}{2} \ \frac{3}{2})$. The summation of (i,n) is limited to those core-excitation admixtures in which at least one $s_{1/2}$ neutron is lifted to the $d_{3/2}$ shell. The summation over (j,m) is limited to core excitations in which only one or two $s_{1/2}$ protons are lifted to the $d_{3/2}$ shell. With this definition, only the

configurations included in the first sum will give rise to $l_n=0$ groups in the (d,p) experiment. It will be assumed that the coefficients are normalized such that

$$\alpha^2 + \sum_{i,n} \beta_{in}^2 + \sum_{j,m} \gamma_{jm}^2 = 1.$$

The observed reduced width for the i th group can be written as

$$\theta_{in}^2 = \beta_{in}^2 S_{in} \theta_0^2 (2s). \quad (2)$$

To estimate the total core-excitation admixture in the ground state of Cl^{35} , the following rough approximation will be made

$$\sum_{i,n} (2J_{in}+1) \theta_{in}^2 = \sum_{i,n} (2J_{in}+1) \beta_{in}^2 S_{in} \theta_0^2 (2s) \approx \langle 2J+1 \rangle_{av} \langle S \rangle_{av} \theta_0^2 (2s) \sum_{i,n} \beta_{in}^2, \quad (3)$$

where $\langle 2J+1 \rangle_{av} \approx 4$, since J is either 1 or 2. The substitution of a "mean spectroscopic factor" $\langle S \rangle_{av}$ for S_{in} was found to be justifiable in this case, since a calculation of a number of S_{in} for $n=1$ and 2 showed that $0.45 \leq S_{in} \leq 1.2$ with $\langle S \rangle_{av} \approx 0.75$. Substitution in Eq. (3) gives

$$\sum_{i,n} \beta_{in}^2 \approx \sum_{i,n} (2J_{in}+1) \theta_{in}^2 / 3\theta_0^2 (2s). \quad (4)$$

A value for $\theta_0^2 (2s) \approx 0.04$ can be estimated from Fig. 56 of reference 15.

Adding the $(2J+1)\theta^2$ values from Table III, column 3, gives

$$\sum_{i,n} (2J_{in}+1) \theta_{in}^2 = 0.03. \quad \text{Thus,} \quad \sum_{i,n} \beta_{in}^2 = 0.25.$$

The value of α^2 can be estimated using a sum rule given in Eq. (III.128) in reference 15. This sum rule allows the calculation of $\sum_J (2J+1) S_J (l=2)$ for the transition given in Fig. 11. The result is $\sum_J = 8$. Summing the values of $(2J+1)\theta^2$ given in Table III, column 4, gives

$$\alpha^2 \sum_J (2J+1) S_J (l=2) \theta_0^2 (1d_{3/2}) = \alpha^2 \sum_J (2J+1) \theta_J^2 (l=2) = 0.064, \quad (5)$$

and therefore

$$\alpha^2 = 0.008 / \theta_0^2.$$

As mentioned above, θ_0^2 can be estimated from Fig. 57 of reference 15 to be about 0.02. Thus, $\alpha^2 \approx 0.4$ and $\sum \gamma_{jm}^2 \approx 0.35$. It is, therefore, concluded that the Cl^{35} ground state contains about 40% $[(d_{3/2}^3)]$; whereas core-excitation admixtures with only $s_{1/2}$ proton holes accounts for about 35%. The remaining 25% is due to proton-neutron holes or neutron holes alone.

The components of $\Psi(\text{Cl}^{35})$ giving rise to the $l_n=0$ admixtures in groups (1) and (0) are of the form

$$[(s_{1/2}^{-1})_{1/2 \ 1/2} (d_{3/2}^4)_{1J}] T_0 J_0 = (\frac{1}{2} \ \frac{3}{2}),$$

with $J=1$ and 2, respectively. The corresponding S values are given in the sixth column of Table III. Using Eq. (2) with $\theta_0(2s)=0.04$, it is found that $\beta^2=0.08$ for $J=2$ and 0.05 for $J=1$.

The observed strong admixture to group (4) (see Sec. III) is not included in the discussion given above.

TABLE III. The $l_n=0$ and $l_n=2$ levels in Cl^{36} .

Level	J	$(2J+1)\theta^2$		$S(d_{3/2})$	$S(s_{1/2})$	$\theta_0^2(d_{3/2})$
		$l_n=0$	$l_n=2$			
0	2^+	0.0021	0.041	16/15	8/15	0.0075
1	3^+	0.0003	0.016	4/15		0.006
2	1^+	0.0053	0.0074	4/15	8/9	0.006
3	$(1,2)^+$	0.0027				
4	$(1,2)^+$	0.013				
6	$(1,2)^+$	0.0034				
31	$(1,2)^+$	0.0030				

Teplov³ assigned $l_n=3$ to this admixture. In this case, level (4) must be a doublet in agreement with the (n, γ) results of Groshev *et al.*⁵

The $l_n=3$ groups observed in Cl^{36} are the groups to levels (7), (9), (10), (13), (20), and (33). Four groups are expected to belong to the shell-model configuration $[(d_{3/2}^3)_{1/2} \ 3/2 (f_{7/2})_{1/2} \ 7/2]_{TJ}$, with $J^\pi = (2, 3, 4, \text{ and } 5)^-$. Since $S=1$ for these transitions, level (7) is probably 5^- , because it has the largest value of $(2J+1)\theta^2$. To determine $\theta_0^2(f_{7/2})$ from the observed $(2J+1)\theta^2$, the sum rule given in Eq. (III.185) of reference 15 was used. This sum rule states that in the "weak coupling" approximation

$$\sum (2J+1)\theta^2 = (2j+1)(2J_0+1)\theta_0^2, \quad (6)$$

where j is the spin of the transferred nucleon. The sum has to be extended over all $l_n=3$, $f_{7/2}$ groups. Since the $f_{7/2}-f_{5/2}$ splitting is about 5 MeV (see reference 11), all observed $l_n=3$ groups are probably $f_{7/2}$. Substitution of the sum of the relevant $(2J+1)\theta^2$ values from Table I into Eq. (6) gives

$$\sum (2J+1)\theta^2 = 0.328 = 32\theta_0^2, \quad (7)$$

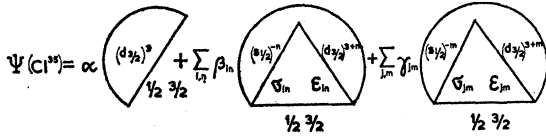


FIG. 12. Ground-state wave function of Cl^{36} .

and thus $\theta_0^2=0.010$, in good agreement with other values found for the $1f$ shell (see reference 15, Fig. 58).

The same sum rule can be used for the $l_n=1$ groups. In this case, however, the sum will include both $p_{3/2}$ and $p_{1/2}$ states, since the $p_{3/2}-p_{1/2}$ splitting is only about 2 MeV.¹¹ The right-hand side of Eq. (6) must therefore be summed over j , which yields

$$\sum (2J+1)\theta^2 = 24\theta_0^2. \quad (8)$$

On summing over the 32 observed $l_n=1$ levels, we find that Eq. (8) gives $24\theta^2=0.58$ if the " $R=5.7 \text{ F}$ " $(2J+1)\theta^2$ values from Table I are used and $24\theta^2=0.96$ if the "adjusted R " values are used. Thus, $0.024 < \theta_0^2 < 0.04$, in reasonable agreement with other estimates in the $2p$ shell (see reference 15, Fig. 59).

Because of the high degree of fragmentation, nothing can be said about the position of the six basic single-particle $2p$ states, which are of the form

$$[(d_{3/2}^3)_{1/2} \ 3/2 (p_j)_{1/2} \ j]_{TJ} \text{ with } j = \frac{1}{2} \text{ and } \frac{3}{2}.$$

Cl^{38}

The ground-state spins of Cl^{37} and Cl^{38} are $\frac{3}{2}^+$ and 2^- , respectively.⁴ According to the shell model, the main component of the ground-state wave function of Cl^{37} is $[(j^n)]_{T_0 J_0} = [(d_{3/2}^5)]_{3/2 \ 3/2}$. The groups (1), (2),

TABLE IV. The $l_n=3$ levels in Cl^{38} .

Level	J	$(2J+1)\theta^2$		$\theta_0^2(f_{7/2})$
		$l_n=1$	$l_n=3$	
0	2^-	?	(≤ 0.14)	(≤ 0.028)
1	5^-		0.20	0.018
2	3^-	0.031	0.070	0.010
3	4^-		0.11	0.012

and (3) (see Table IV) can be ascribed to the transitions indicated in Fig. 13, where J^π can be equal to 2^- , 3^- , 4^- , and 5^- . Although the $l_n=3$ nature of the ground state could not be established in this work for experimental reasons, the ground state will be assumed to be the $J^\pi=2^-$, $f_{7/2}$ level. According to their spin values, the $J^\pi=2^-$ and 3^- levels can be admixed with $l_n=1$. Because level (2) has a strong $l_n=1$ admixture, while levels (1) and (3) are probably pure $l_n=3$, level (2) must have $J=3^-$. For the transitions indicated diagrammatically in Fig. 13, $S=1$. Thus, the ratios of the $(2J+1)\theta^2$ for the levels with $J=3, 4$, and 5 must be $7:9:11$. The observed ratios are $6:9:16$ for the levels (2), (3), and (1), respectively. Therefore, level (3) is 4^- , and level (1) is 5^- . These assignments are in excellent agreement with the prediction from known excitation energies and spins in K^{40} .¹⁸ The values of $\theta_0^2(f_{7/2})$ are given in the last column of Table IV. They agree reasonably well with other values found for this subshell (see reference 15, Fig. 58). The $l_n=1$ admixture to level (2) is about 40%. This admixture is due to an interaction with the appropriate $2p_{3/2}$ level. Since the ratio $\theta_0^2(2p)/\theta_0^2(1f) \approx 2$ (see reference 15, Figs. 58 and 59), the configuration admixture is only 20%. This admixture can be produced with a matrix element of the order of 500 keV, as follows from first-order perturbation theory.¹⁹ A calculation of this matrix element by Pandya and French²⁰ yields 320 keV.

The four strong $l_n=1$ groups (4), (6), (7), and (9) can be ascribed to the transitions shown in Fig. 14, where J^π can be equal to 0^- , 1^- , 2^- , and 3^- . Using the sum rule given in Eq. (6) and the observed $(2J+1)\theta^2$ values for "adjusted R " from Table II, $\theta_0^2(2p_{3/2})$ is found to be 0.028, in good agreement with other values for this subshell given in Fig. 59 of reference 15. Since

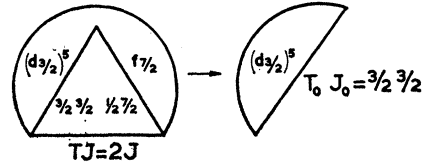
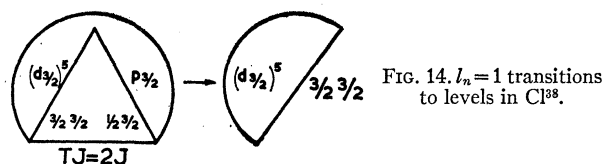


FIG. 13. $l_n=3$ transitions to levels in Cl^{38} .

¹⁸ I. Talmi and I. Unna, *Ann. Rev. Nuclear Sci.* **10**, 372 (1960).

¹⁹ J. B. French, *Nuclear Spectroscopy*, edited by F. Ajzenberg-Selove (Academic Press Inc., New York, 1960), p. 918.

²⁰ S. P. Pandya and J. B. French, *Ann. Phys. (New York)* **2**, 166 (1957).

FIG. 14. $l_n=1$ transitions to levels in Cl^{38} .

$S=1$, the $(2J+1)\theta^2$ values are expected to be in the proportion of 1:3:5:7 for $J=0, 1, 2$, and 3, respectively. The observed ratio is 1.7:4.5:5:6 for the levels (7), (6), (4), and (9), respectively. Therefore, the most probable spin assignments are as given in Table V. The values of $\theta_0^2(2p)$ using these spin values are given in column 4 of this table.

Contrary to the situation in Cl^{36} , no other strong $l_n=1$ groups have been observed in Cl^{38} in the region below $E_x=3.5$ MeV. Thus, in contrast to the situation in Cl^{36} , the $2p_{3/2}$ levels in Cl^{38} show no strong fragmentation. This might well be due to the closed $d_{3/2}$ neutron subshell in Cl^{38} . The $2p_{1/2}$ levels are not observed. They

TABLE V. The $l_n=1$ levels in Cl^{38} .

Level	J	$(2J+1)\theta^2$	$\theta_0^2(2p)$
4	2^-	0.129	0.026
6	1^-	0.118	0.037
7	0^-	0.045	0.045
9	3^-	0.156	0.022

have probably excitation energies higher than 3.5 MeV. Indeed, at about 3.8 MeV, a strong indication was found of Cl^{38} groups; however, the large Cl^{36} level density in this region obstructed the analysis.

ACKNOWLEDGMENTS

At the time this work was undertaken, one of the authors (A. M. H.) was a Sloan Postdoctoral Fellow in the M.I.T. School for Advanced Study, and another (E. K.) was sponsored by the postdoctoral program of the National Science Foundation.